

AnyV2V: A Plug-and-Play Framework For Any Video-to-Video Editing Tasks

Max Ku^{1,2} *, Cong Wei^{1,2*}, Weiming Ren^{1,2*}, Harry Yang³, and Wenhui Chen^{1,2}

¹ University of Waterloo

² Vector Institute, Toronto

³ Harmony.AI

{m3ku, c58wei, w2ren, wenhuchen}@uwaterloo.ca

<https://tiger-ai-lab.github.io/AnyV2V/>

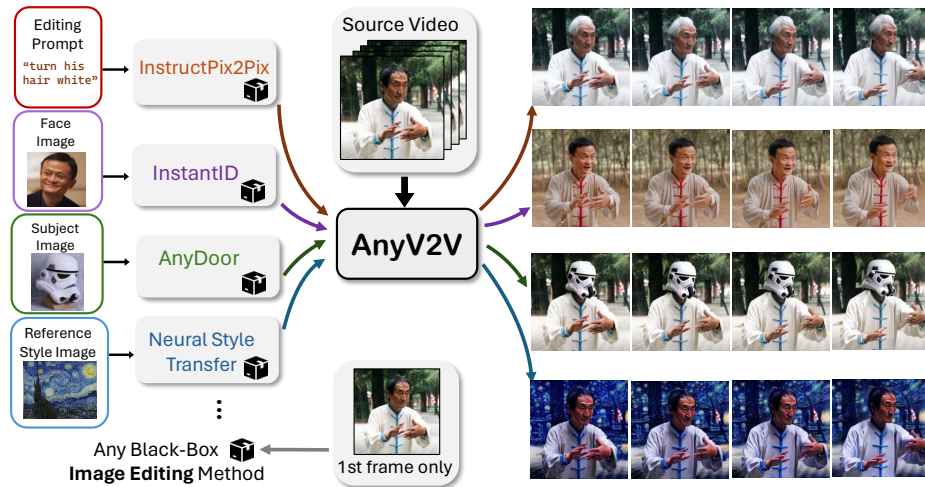


Fig. 1: We build a universal framework AnyV2V to handle all types of video-to-video editing tasks conditioned on different inputs. AnyV2V disentangles the video editing process into two stages: (1) first-frame image editing and (2) image-to-video generation with DDIM inversion + feature injection.

Abstract. Video-to-video editing involves editing a source video along with additional control (such as text prompts, subjects, or styles) to generate a new video that aligns with the source video and the provided control. Traditional methods have been constrained to certain editing types, limiting their ability to meet the wide range of user demands. In this paper, we introduce AnyV2V, a novel training-free framework designed to simplify video editing into two primary steps: (1) employing an off-the-shelf image editing model (e.g. InstructPix2Pix, InstantID, etc)

* These authors contributed equally to this work.

to modify the first frame, (2) utilizing an existing image-to-video generation model (e.g. I2VGen-XL) for DDIM inversion and feature injection. In the first stage, AnyV2V can plug in any existing image editing tools to support an extensive array of video editing tasks. Beyond the traditional prompt-based editing methods [15, 20, 23, 36, 54, 55], AnyV2V also can support novel video editing tasks, including reference-based style transfer, subject-driven editing, and identity manipulation, which were unattainable by previous methods. In the second stage, AnyV2V can plug in any existing image-to-video models to perform DDIM inversion and intermediate feature injection to maintain the appearance and motion consistency with the source video. On the prompt-based editing, we show that AnyV2V can outperform the previous best approach by 35% on prompt alignment, and 25% on human preference. On the three novel tasks, we show that AnyV2V also achieves a high success rate. We believe AnyV2V will continue to thrive due to its ability to seamlessly integrate the fast-evolving image editing methods. Such compatibility can help AnyV2V to increase its versatility to cater to diverse user demands.

Keywords: video editing · diffusion models · plug-and-play

1 Introduction

The task of video-to-video editing represents a crucial area of research that enables users to edit and create videos according to their preferences seamlessly. In this domain, an AI model is tasked with processing a source video along with various forms of guidance—such as text prompts, facial identity, styles, subjects, depth, and more—to synthesize a new video. It is imperative that the synthesized video not only remains faithful to the source video but also accurately incorporates the additional guidance provided. This requirement ensures that the synthesized video meets the specific desires and intentions of the user. In order to tackle the video-to-video generation tasks, an extensive range of methods [3, 15, 15, 20, 23, 35, 36, 54, 55] have been proposed. These methods are built on top of the open-source image or video diffusion models [9, 17, 45, 53, 62]. However, these methods are all limited to performing specific types of editing tasks. For instance, TokenFlow [20] excels at text-guided style transfer but falls short in localized editing. VideoP2P [36] are restricted to follow certain types of editing prompts. Besides, some of these approaches [17, 23, 55] require additional parameter tuning or video feature extraction (e.g. tracking, point correspondence, etc) to ensure appearance or temporal consistency. Such overhead could lead to much higher time and memory costs. These limitations make them incapable of meeting the diverse user requirements, necessitating the establishment of separate video editing workflows for different tasks.

In recognition of these limitations, a compelling need arises to conceptualize and develop a simple and general-purpose video editing solution. In this paper, we introduce a unified yet simple framework, AnyV2V, designed to address (possibly) any video editing tasks. Our primary insight is that any video editing task can be effectively decomposed into two pivotal stages:

1. Apply an off-the-shelf task-specific image editing model over the first frame.
2. Apply an image-to-video model to perform DDIM inversion on the source video and then inject the intermediate features to generate the new video.

In the first stage, AnyV2V employs an existing task-specific image editing method to edit the first frame (Section 4.1). In the second stage, we aim to propagate the edited effect across the entire video while ensuring alignment with the source video. To achieve this, we follow an invert-and-generate framework [38, 56]. In contrast to prior methods that employed text-to-video models [3, 4] for DDIM inversion [47], we employ the image-to-video models [12, 44, 62] for DDIM inversion (Section 4.2) to enable the first-frame condition. With the inverted latents as initial noise and the modified first frame as the conditional signal, the I2V model is able to generate videos that are not only faithful to the edited first frame but also follow the appearance and motion of the source video. To further enforce the consistency of the appearance and motion with the source video, we perform feature injection in convolution layers, spatial attention layers and temporal attention layers in the denoising U-Net of the I2V model. These techniques are discussed in detail in Section 4.3 and Section 4.4, and we demonstrate their effectiveness by conducting an ablation study in Section 5.5. By performing the two-stage editing process, AnyV2V effectively offloads the editing operation to existing image editing tools. This disentanglement helps AnyV2V excel in:

1. **Compatibility:** AnyV2V has superior compatibility with all the image editing methods. We demonstrate that AnyV2V can seamlessly build on top of advanced image editing methods, such as InstructPix2Pix [6], InstantID [51], NST [18], AnyDoor [11] to perform diverse types of editing.
2. **Simplicity:** AnyV2V is a tuning-free approach without requiring any additional video features to achieve high appearance and temporal consistency.

In this paper, we showcase AnyV2V’s versatility and effectiveness by the qualitative and quantitative results. We comprehensively evaluate our method on four important tasks: (1) prompt-based editing, (2) reference-based style transfer, (3) subject-driven editing and (4) identity manipulation. We collected a new dataset of roughly 100 examples based on the four tasks to evaluate the performance of AnyV2V and other baselines [15, 20, 55]. We show that AnyV2V is among the first to perform (2) reference-based style transfer, (3) subject-driven editing, and (4) identity manipulation in the video domain. Moreover, the AnyV2V exhibits 25% human preference improvement over the previous best model [20] in (1) prompt-based editing. We also perform a comprehensive ablation study to show the impact of our design choices. Our contributions are summarized as follows:

1. We introduce AnyV2V, a plug-and-play unified framework tailored for a diverse range of video-to-video editing tasks.
2. To the best of our knowledge, we are the first to perform video editing using pre-trained I2V models, marking a novel paradigm in this field.
3. Universal compatibility with image editing methods. AnyV2V is compatible with any image editing method, extending any image editing method into the video domain at no cost.

4. We show, both quantitatively and qualitatively, that our method outperforms existing state-of-the-art baselines on prompt-based editing and exhibits robust performance on three novel tasks: reference-based style transfer, subject-driven editing, and identity manipulation.

2 Related Work

Text-to-Video (T2V) Generation. Recent advancements in diffusion models [27, 46] have led to a huge development in text-to-video (T2V) generation. Existing diffusion-based T2V models generally follow the paradigm of extending text-to-image (T2I) generation models to the video domain, where additional temporal modelling layers are added to the T2I model to enable video generation. Recent T2V generation models are developed from pixel-space diffusion models [19, 26, 29], latent diffusion models (LDMs) [1, 5, 8, 24, 53, 63], as well as diffusion transformers [10, 25, 41]. LDM-based [45] T2V generation models are the most extensively studied methods due to their high efficiency and the open-sourced Stable Diffusion [45] models. T2V models have been shown to be foundational models for a wide range of applications such as I2V generation [57], personalized video generation [39] and video editing [3].

Image-to-Video (I2V) Generation. To achieve more precise control over the video generation process, a series of I2V generation methods employing additional image conditions in the video generation process have emerged. Earlier efforts such as VideoComposer [52] and VideoCrafter1 [8] use the input image as a style reference and cannot fully preserve the visual details in the output videos. More recently, methods such as DynamiCrafter [57], I2VGen-XL [62], SEINE [12] and ConsistI2V [44] have overcome this problem and can generate videos that are more consistent with the input image (often used as the first frame of the video). I2V generation models have also been employed in a wide range of applications such as long video generation [12, 44, 59], generative frame interpolation [12, 57] and video storytelling [57, 59]. However, to the best of our knowledge, no methods have applied I2V generation models for video editing. We aim to investigate this area and propose a highly flexible training-free framework for video editing using I2V generation models.

Semantic Image and Video Editing. Visual generation has attracted considerable attention within the field; however, visual manipulation also represents a significant and popular area of interest. The research area of image editing encompasses a wide range of tasks. The popular tasks include stylization [13, 18, 37], identity manipulation [51], subject-driven editing [11, 22, 34], and localized editing [2, 33, 40, 48]. One interesting direction is to train a model to understand text inputs to perform general image editing tasks [6, 49, 60]. However, image editing remained an open and challenging problem as none of the work was able to tackle all the tasks effectively [31]. On the other hand, the video editing problem

was often perceived as an extension of image editing problems, incorporating the time dimension. Recent video editing works [7, 15, 20, 42, 54, 58] employ text prompts to execute video editing tasks. These approaches have opened new avenues for interactive and intuitive video manipulation, allowing users to guide the editing process through natural language. However, such methodologies fail to offer precise control to the user, often resulting in edits that may not fully align with the user’s intentions or the desired level of detail due to the ambiguity of natural language and the limit of model capability. Our work is the first to enable precise video editing using pre-trained Image-to-Video (I2V) models. More importantly, our paradigm merges the two problems into a single domain to create a unified solution, offering high controllability in video editing tasks.

3 Preliminary

Image-to-Video (I2V) Generation Models. In this work, we focus on leveraging latent diffusion-based [45] I2V generation models for video editing. Given an input first frame I_1 , a text prompt \mathbf{s} and a noisy video latent \mathbf{z}_t at time step t , I2V generation models recover a less noisy latent \mathbf{z}_{t-1} using a denoising model $\epsilon_\theta(\mathbf{z}_t, I_1, \mathbf{s}, t)$ conditioned on both I_1 and \mathbf{s} . The denoising model ϵ_θ contains a set of spatial and temporal self-attention layers, where the self-attention operation can be formulated as:

$$Q = W^Q z, K = W^K z, V = W^V z, \quad (1)$$

$$\text{Attention}(Q, K, V) = \text{Softmax}\left(\frac{QK^\top}{\sqrt{d}}\right)V, \quad (2)$$

where z is the input hidden state to the self-attention layer and W^Q , W^K and W^V are learnable projection matrices that map z onto query, key and value vectors, respectively. For spatial self-attention, z represents a sequence of spatial tokens from each frame. For temporal self-attention, z is composed of tokens located at the same spatial position across all frames.

DDIM Inversion. The denoising process for I2V generation models from \mathbf{z}_t to \mathbf{z}_{t-1} can be achieved using the DDIM [47] sampling algorithm. The reverse process of DDIM sampling, known as DDIM inversion [16, 38], allows obtaining \mathbf{z}_{t+1} from \mathbf{z}_t such that $\mathbf{z}_{t+1} = \sqrt{\frac{\alpha_{t+1}}{\alpha_t}} \mathbf{z}_t + \left(\sqrt{\frac{1}{\alpha_{t+1}} - 1} - \sqrt{\frac{1}{\alpha_t} - 1}\right) \cdot \epsilon_\theta(\mathbf{z}_t, x_0, \mathbf{s}, t)$, where α_t is derived from the variance schedule of the diffusion process.

Plug-and-Play (PnP) Diffusion Features. Tumanyan et al. [49] proposed PnP diffusion features for image editing, based on the observation that intermediate convolution features f and self-attention scores $A = \text{Softmax}\left(\frac{QK^\top}{\sqrt{d}}\right)$ in a text-to-image (T2I) denoising U-Net capture the semantic regions (e.g. legs or torso of a human body) during the image generation process.

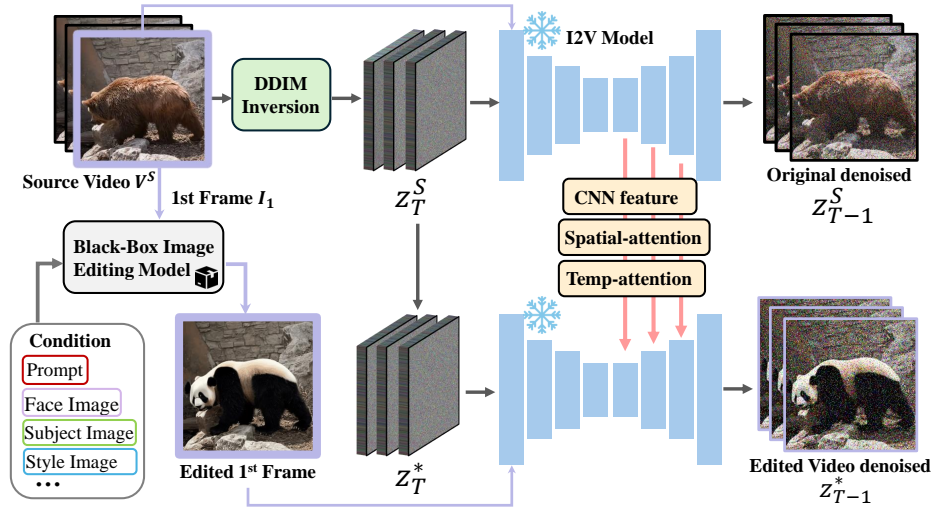


Fig. 2: AnyV2V framework. Our framework takes a source video V^S as input. In the first stage, we apply a block-box image editing method on the first frame I_1 according to the editing task. In the second stage, the source video is inverted to initial noise z_T^S , which is then denoised using DDIM sampling. During the sampling process, we extract spatial features, spatial attention, and temporal attention from the image-to-video models’ decoder layers. To generate our edited video, we perform a DDIM sampling by fixing z_T^* as z_T^S and use the edited first frame as the conditional signal. During the sampling, we inject the features and attention into corresponding layers of the model.

Given an input source image I^S and a target prompt P , PnP first performs DDIM inversion to obtain the image’s corresponding noise $\{z_t^S\}_{t=1}^T$ at each time step t . It then collects the convolution features $\{f_t^l\}$ and attention scores $\{A_t^l\}$ from some predefined layers l at each time step t of the backward diffusion process $z_{t-1}^S = \epsilon_\theta(z_t^S, \emptyset, t)$, where \emptyset denotes the null text prompt during denoising.

To generate the edited image I^* , PnP starts from the initial noise of the source image (i.e. $z_T^* = z_T^S$) and performs feature injection during denoising: $z_{t-1}^* = \epsilon_\theta(z_t^*, P, t, \{f_t^l, A_t^l\})$, where $\epsilon_\theta(\cdot, \cdot, \cdot, \{f_t^l, A_t^l\})$ represents the operation of replacing the intermediate feature and attention scores $\{f_t^{l*}, A_t^{l*}\}$ with $\{f_t^l, A_t^l\}$. This feature injection mechanism ensures I^* to preserve the layout and structure from I^S while reflecting the description in P . To control the feature injection strength, PnP also employs two thresholds τ_f and τ_A such that the feature and attention scores are only injected in the first τ_f and τ_A denoising steps. Our method extends this feature injection mechanism to I2V generation models, where we inject features in convolution, spatial, and temporal attention layers. We show the detailed design of AnyV2V in Section 4.

4 AnyV2V

Our method presents a two-stage approach to video editing. Given a source video $V^S = \{I_1, I_2, I_3, \dots, I_n\}$, where I_i is the frame at time i and n denotes the video length. We extract the initial frame I_1 and pass it into an image editing model ϕ_{img} to obtain an edited first frame $I_1^* = \phi_{\text{img}}(I_1, C)$, where C is the auxiliary conditions for image editing models such as text prompt, mask, style, etc. In the second stage, we feed the edited first frame I_1^* and a target prompt \mathbf{s}^* into an I2V generation model ϵ_θ and employ the inverted latent from the source video V^S to guide the generation process such that the edited video V^* follows the motion of the source video V^S and the semantic information represented in the edited first frame I_1^* and the target prompt \mathbf{s}^* . An overall illustration of our video editing pipeline is shown in Figure 2. In this section, we explain each core component of our method.

4.1 Flexible First Frame Editing

In visual manipulation, controllability is a key element in performing precise editing. Current video editing models lack this controllability as most of the existing methods can only edit videos based on target text prompts (e.g. TokenFlow [20]) or text instructions (e.g. InsV2V [14]). Our AnyV2V enables more controllable video editing by utilizing image editing models to modify the video’s first frame. This strategic approach enables highly accurate modifications in the video and is compatible with a broad spectrum of image editing models, including other deep learning models that can perform image style transfer [18, 21, 37], mask-based image editing [2, 40], image inpainting [33, 48], identity-preserving image editing [51], and subject-driven image editing [11, 22, 34]. This stage is highly flexible and it can even be done by human experts.

4.2 Structural Guidance using DDIM Inversion

To ensure the generated videos from the I2V generation model follow the general structure as presented in the source video, we employ DDIM inversion to obtain the latent noise of the source video at each time step t . Specifically, we perform the inversion *without* text prompt condition but *with* the first frame condition. Formally, given a source video $V^S = \{I_1, I_2, I_3, \dots, I_n\}$, we obtain the inverted latent noise for time step t as:

$$\mathbf{z}_t^S = \text{DDIM_Inv}(\epsilon_\theta(\mathbf{z}_{t+1}, I_1, \emptyset, t)), \quad (3)$$

where $\text{DDIM_Inv}(\cdot)$ denotes the DDIM inversion operation as described in Section 3. In ideal cases, the latent noise \mathbf{z}_T^S at the final time step T (initial noise of the source video) should be used as the initial noise for sampling the edited videos. In practice, we find that due to the limited capability of certain I2V models, the edited videos denoised from the last time step are sometimes distorted. Following [34], we observe that starting the sampling from a previous time step $T' < T$ can be used as a simple workaround to fix this issue.

4.3 Appearance Guidance via Spatial Feature Injection

Our empirical observation (*cf.* Section 5.5) suggests that I2V generation models already have some editing capabilities by only using the edited first frame and DDIM inverted noise as the model input. However, we find that this simple approach is often unable to correctly preserve the background in the edited first frame and the motion in the source video, as the conditional signal from the source video encoded in the inverted noise is limited.

To enforce consistency with the source video, we perform feature injection in both convolution layers and spatial attention layers in the denoising U-Net. During the video sampling process, we simultaneously denoise the source video using the previously collected DDIM inverted latents \mathbf{z}_t^S at each time step t such that $\mathbf{z}_{t-1}^S = \epsilon_\theta(\mathbf{z}_t^S, I_1, \emptyset, t)$. We preserve two types of hidden features during source video denoising: convolution features f^{l_1} before skip connection from the l_1^{th} residual block in the U-Net decoder, and the spatial self-attention scores $\{A_s^{l_2}\}$ from $l_2 = \{l_{low}, l_{low+1}, \dots, l_{high}\}$ layers. We collect the queries $\{Q_s^{l_2}\}$ and keys $\{K_s^{l_2}\}$ instead of directly collecting $A_s^{l_2}$ as the attention score matrices are parameterized by the query and key vectors. We then replace the corresponding features during denoising the edited video in both the normal denoising branch and the negative prompt branch for classifier-free guidance [28]. We use two thresholds τ_{conv} and τ_{sa} to control the convolution and spatial attention injection to only happen in the first τ_{conv} and τ_{sa} steps during video sampling.

4.4 Motion Guidance through Temporal Feature Injection

The spatial feature injection mechanism described in Section 4.3 significantly enhances the background and overall structure consistency of the edited video. While it also helps maintain the source video motion to some degree, we observe that the edited videos will still have a high chance of containing incorrect motion compared to the source video. On the other hand, we notice that I2V generation models, or video diffusion models in general, are often initialized from pre-trained T2I models and continue to be trained on video data. During the training process, parameters in the spatial layers are often frozen or set to a lower learning rate such that the pre-trained weights from the T2I model are less affected, and the parameters in the temporal layers are more extensively updated during training. Therefore, it is likely that a large portion of the motion information is encoded in the temporal layers of the I2V generation models. Concurrent work [3] also observes that features in the temporal layers show similar characteristics with optical flow [30], a pattern that is often used to describe the motion of the video.

To better reconstruct the source video motion in the edited video, we propose to also inject the temporal attention features in the video generation process. Similar to spatial attention injection, we collect the source video temporal self-attention queries $Q_t^{l_3}$ and keys $K_t^{l_3}$ from some U-Net decoder layers represented by l_3 and inject them into the edited video denoising branches. We also only apply temporal attention injection in the first τ_{ta} steps during sampling. Overall,

combining the spatial and temporal feature injection mechanisms, the denoising process of our AnyV2V can be represented by:

$$\mathbf{z}_{t-1}^* = \epsilon_{\theta}(\mathbf{z}_t^*, I^*, \mathbf{s}^*, t, \{f^{l_1}, Q_s^{l_2}, K_s^{l_2}, Q_t^{l_3}, K_t^{l_3}\}). \quad (4)$$

Our proposed spatial and temporal feature injection scheme enables tuning-free adaptation of I2V generation models for video editing. Our experimental results demonstrate that each component in our design is crucial to the accurate editing of source videos. We showcase more qualitative results for the effectiveness of our model components in Section 5.

5 Experiments

In this section, we first introduce four video editing tasks that we focus on evaluating our AnyV2V framework: (1) prompt-based editing, (2) reference-based style transfer, (3) subject-driven editing, and (4) identity manipulation. We then assess the effectiveness of AnyV2V both quantitatively and qualitatively on these four tasks. For (1) prompt-based editing, we compare AnyV2V with SoTA text-guided video editing baselines. For the three novel tasks (2)(3)(4), as these tasks require reference images to guide video editing, current text-based video editing methods are incapable of performing such edits. We thus compare the performance of AnyV2V using different I2V generation backbones.

5.1 Tasks Definition

1. **Prompt-based Editing:** allows users to manipulate video content using only natural language. This can include descriptive prompts or instructions. With the prompt, Users can perform a wide range of edits, such as incorporating accessories, spawning or swapping objects, adding effects, or altering the background.
2. **Reference-based Style Transfer:** In the realm of style transfer tasks, the artistic styles of Monet and Van Gogh are frequently explored, but in real-life examples, users might want to use a distinct style based on one particular artwork. In reference-based style transfer, we focus on using a style image as a reference to perform video editing. The edited video should capture the distinct style of the referenced artwork.
3. **Subject-driven Editing:** In subject-driven video editing, we aim at replacing an object in the video with a target subject based on a given subject image while maintaining the video motion and persevering the background.
4. **Identity Manipulation:** Identity manipulation allows the user to manipulate video content by replacing a person with another person’s identity in the video based on an input image of the target person.

5.2 Implementation Details

We employ AnyV2V on three off-the-shelf I2V generation models: I2VGen-XL⁴ [62], ConsistI2V [44] and SEINE [12]. For all I2V models, we use $\tau_{conv} = 0.2T$, $\tau_{sa} = 0.2T$ and $\tau_{ta} = 0.5T$, where T is the total number of sampling steps. We use the DDIM [47] sampler and set T to the default values of the selected I2V models. Following PnP [50], we set $l_1 = 4$ for convolution feature injection and $l_2 = l_3 = \{4, 5, 6, \dots, 11\}$ for spatial and temporal attention injections. During sampling, we apply text classifier-free guidance (CFG) [28] for all models with the same negative prompt “*Distorted, discontinuous, Ugly, blurry, low resolution, motionless, static, disfigured, disconnected limbs, Ugly faces, incomplete arms*” across all edits. We refer readers to the supplementary materials for more discussions on our implementation details and hyperparameter settings.

To obtain the initial edited frames in our implementation, we use a set of image editing model candidates including prompt-based image editing model InstructPix2Pix [6], style transfer model Neural Style Transfer (NST) [18], subject-driven image editing model AnyDoor [11], and identity-driven image editing model InstantID [51]. We experiment with only the successfully edited frames, which is crucial for our method.

5.3 Quantitative Evaluations

Prompt-based Editing. For (1) prompt-based editing, we conduct a human evaluation to examine the degree of prompt alignment and overall preference of the edited videos based on user voting. We compare AnyV2V against three baseline models: Tune-A-Video [55], TokenFlow [20] and FLATTEN [15]. Human evaluation results in Table 1 demonstrate that our model achieves the best overall preference and prompt alignment among all methods, and AnyV2V (I2VGen-XL) is the most preferred method. We conjecture that the gain is coming from our compatibility with state-of-the-art image editing models.

We also employ automatic evaluation metrics on our edited video of the human evaluation datasets. Following previous works [3, 7], our automatic evaluation employs the CLIP [43] model to assess both text alignment and temporal consistency. For text alignment, we calculate the CLIP-Score, specifically by determining the average cosine similarity between the CLIP text embeddings derived from the editing prompt and the CLIP image embeddings across all frames. For temporal consistency, we evaluate the average cosine similarity between the CLIP image embeddings of every pair of consecutive frames. These two metrics are referred to as CLIP-Text and CLIP-Image, respectively. Our automatic evaluations in Table 1 demonstrate that our model is competitive in prompt-based editing compared to baseline methods.

Reference-based Style Transfer; Identity Manipulation and Subject-driven Editing For novel tasks (2),(3) and (4), we evaluate the performance

⁴ We use the version provided in <https://huggingface.co/ali-vilab/i2vgen-xl>.

Table 1: Quantitative comparisons for our AnyV2V with baselines on prompt-based video editing tasks. Alignment: prompt alignment; Overall: overall preference. **Bold:** best results; Underline: top-2.

Task	Prompt-based Editing			
Method	Human Evaluation \uparrow		CLIP Scores \uparrow	
	Alignment	Overall	CLIP-Text	CLIP-Image
Tune-A-Video [55]	15.2%	2.1%	0.2902	0.9704
TokenFlow [20]	31.7%	<u>20.7%</u>	0.2858	0.9783
FLATTEN [15]	25.5%	16.6%	0.2742	<u>0.9739</u>
AnyV2V (SEINE)	28.9%	8.3%	<u>0.2910</u>	0.9631
AnyV2V (ConsistI2V)	<u>33.8%</u>	11.7%	0.2896	0.9556
AnyV2V (I2VGen-XL)	69.7%	46.2%	0.2932	0.9652

Table 2: Comparisons for three I2V models under AnyV2V framework on novel video editing tasks. Align: reference alignment; Overall: overall preference. **Bold:** best results; Underline: top-2.

Task	Reference-based Style Transfer	Subject-driven Editing	Identity Manipulation
Image Editing Method	NST [18]	AnyDoor [11]	InstantID [51]
Image Editing Success Rate	$\approx 90\%$	$\approx 10\%$	$\approx 80\%$
Human Evaluation	Align \uparrow Overall \uparrow	Align \uparrow Overall \uparrow	Align \uparrow Overall \uparrow
AnyV2V (SEINE)	<u>92.3%</u> <u>30.8%</u>	48.4% 15.2%	<u>72.7%</u> 18.2%
AnyV2V (ConsistI2V)	38.4% 10.3%	<u>63.6%</u> <u>42.4%</u>	<u>72.7%</u> <u>27.3%</u>
AnyV2V (I2VGen-XL)	100.0% 76.9%	93.9% 84.8%	90.1% 45.4%

of three I2V generation models using human evaluations and show the results in Table 2. As these tasks require reference images instead of text prompts, we focus on evaluating the reference alignment and overall preference of the edited videos. According to the results, we observe that AnyV2V (I2VGen-XL) is the best model across all tasks, underscoring its robustness and versatility in handling diverse video editing tasks. AnyV2V (SEINE) and AnyV2V (ConsistI2V) show varied performance across tasks. AnyV2V (SEINE) performs good reference alignment in reference-based style transfer and identity manipulation, but falls short in subject-driven editing with lower scores. On the other hand, AnyV2V (ConsistI2V) shines in subject-driven editing, achieving second-best results in both reference alignment and overall preference. Since the latest image editing models have not yet reached a level of maturity that allows for consistent and precise editing [32], we also report the image editing success rate in Table 2 to clarify that our method relies on a good image frame edit.

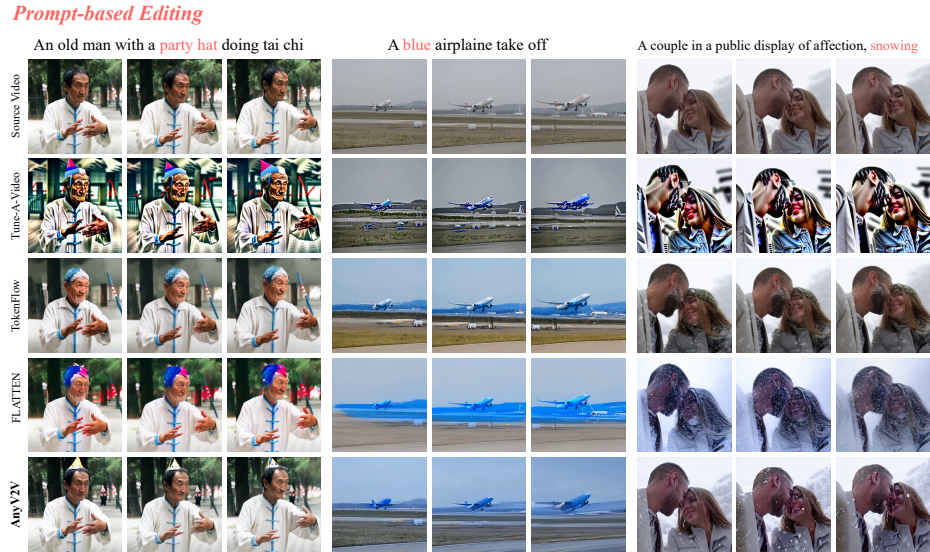


Fig. 3: AnyV2V is robust in a wide range of prompt-based editing tasks while maintaining the background. The generated results align the most with the text prompt and also maintain high motion consistency.

5.4 Qualitative Results

Prompt-based Editing. By leveraging the strength of image editing models, our AnyV2V framework provides precise control of the edits such that the irrelevant parts in the scene are untouched after editing. In our experiment, we used InstructPix2Pix [6] for the first frame edit. Shown in Figure 3, our method correctly places a party hat on an old man’s head and successfully turns the color of an airplane to blue, while preserving the background and keeping the fidelity to the source video. Comparing our work with the three baseline models TokenFlow [20], FLATTEN [15], and Tune-A-Video [55], the baseline methods display either excessive or insufficient changes in the edited video to align with the editing text prompt. The color tone and object shapes are also tilted. It is also worth mentioning that our approach is far more consistent on some motion tasks such as adding snowing weather, due to the I2V model’s inherent support for animating still scenes. The baseline methods, on the other hand, can add snow to individual frames but cannot generate the effect of snow falling, as the per-frame or one-shot editing methods lack the ability of temporal modelling.

Reference-based Style Transfer. Our approach diverges from relying solely on textual descriptors for conducting style edits, using the style transfer model NST [18] to obtain the edited frame. This level of controllability offers artists the unprecedented opportunity to use their art as a reference for video editing, opening new avenues for creative expression. As demonstrated in Figure 4,

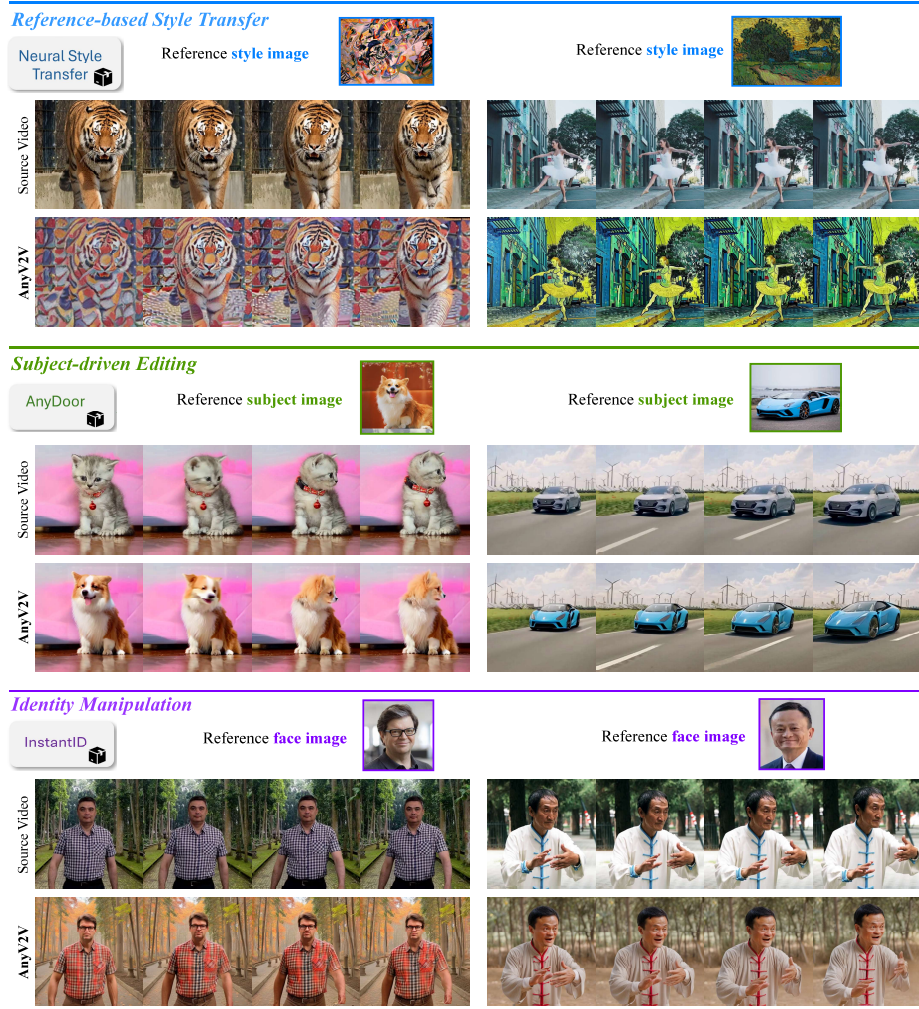


Fig. 4: With different image editing models, AnyV2V can achieve a wide range of editing tasks, including reference-based style transfer, subject-driven editing, and identity manipulation.

our method captures the distinctive style of Vassily Kandinsky’s artwork “Composition VII” and Vincent Van Gogh’s artwork “Chateau in Auvers at Sunset” accurately, while such an edit is often hard to perform using existing text-guided video editing methods.

Subject-driven Editing. In our experiment, we employed a subject-driven image editing model AnyDoor [11] for the first frame editing. AnyDoor allows replacing any object in the target image with the subject from only one refer-

Table 3: Ablation study results for AnyV2V (I2VGen-XL). T. Injection and S. Injection correspond to temporal and spatial feature injection mechanisms, respectively.

Model	CLIP-Image \uparrow
AnyV2V (I2VGen-XL)	0.9648
AnyV2V (I2VGen-XL) w/o T. Injection	0.9652
AnyV2V (I2VGen-XL) w/o T. Injection & S. Injection	0.9637
AnyV2V (I2VGen-XL) w/o T. Injection & S. Injection & DDIM Inversion	0.9607

ence image. We observe from Figure 4 that AnyV2V produces highly motion-consistent videos when performing subject-driven object swapping. In the first example, AnyV2V successfully replaces the cat with a dog according to the reference image and maintains highly aligned motion and background as reflected in the source video. In the second example, the car is replaced by our desired car while maintaining the rotation angle in the edited video.

Identity Manipulation. By integrating the identity-preserved image personalization model InstantID [51] with ControlNet [61], this approach enables the replacement of an individual’s identity to create an initial frame. Our AnyV2V framework then processes this initial frame to produce an edited video, swapping the person’s identity as showcased in Figure 4. To the best of our knowledge, our work is the first to provide such flexibility in the video editing models. Note that the InstantID with ControlNet method will alter the background due to its model property. It is possible to leverage other identity-preserved image personalization models and apply them to AnyV2V to preserve the background.

5.5 Ablation Study

To verify the effectiveness of our design choices, we conduct an ablation study by iteratively disabling the three core components in our model: temporal feature injection, spatial feature injection, and DDIM inverted latent as initial noise. We use AnyV2V (I2VGen-XL) and a subset of 20 samples in this ablation study and report both the frame-wise consistency results using CLIP-Image score in Table 3 and qualitative comparisons in Figure 5. We provide more ablation analysis of other design considerations of our model in the supplementary materials.

Effectiveness of Temporal Feature Injection. According to the results, after disabling temporal feature injection in AnyV2V (I2VGen-XL), while we observe a slight increase in the CLIP-Image score value, the edited videos often demonstrate less adherence to the motion presented in the source video. For example, in the second frame of the “couple sitting” case (3rd row, 2nd column in the right panel in Figure 5), the motion of the woman raising her leg in the source video is not reflected in the edited video without applying temporal injection. On the other hand, even when the style of the video is completely changed, AnyV2V (I2VGen-XL) with temporal injection is still able to capture this nuance motion in the edited video.

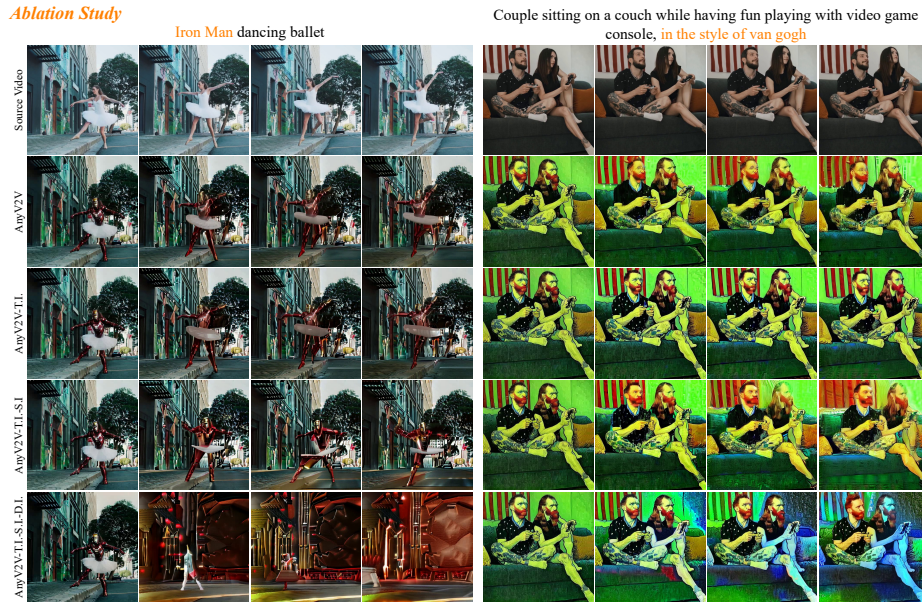


Fig. 5: Visual comparisons of AnyV2V’s editing results after disabling temporal feature injection (T.I.), spatial feature injection (S.I.) and DDIM inverted initial noise (D.I.).

Effectiveness of Spatial Feature Injection. As shown in Table 3, we observe a drop in the CLIP-Image score after removing the spatial feature injection mechanisms from our model, indicating that the edited videos are not smoothly progressed across consecutive frames and contain more appearance and motion inconsistencies. Further illustrated in the third row of Figure 5, removing spatial feature injection will often result in incorrect subject appearance and pose (as shown in the “ballet dancing” case) and degenerated background appearance (evident in the “couple sitting” case). These observations demonstrate that directly generating edited videos from the DDIM inverted noise is often not enough to fully preserve the source video structures, and the spatial feature injection mechanisms are crucial for achieving better editing results.

DDIM Inverted Noise as Structural Guidance. Finally, we observe a further decrease in CLIP-Image scores and a significantly degraded visual appearance in both examples in Figure 5 after replacing the initial DDIM inverted noise with random noise during sampling. This indicates that the I2V generation models become less capable of animating the input image when the editing prompt is completely out-of-domain and highlights the importance of the DDIM inverted noise as the structural guidance of the edited videos.

6 Conclusion

In this paper, we present AnyV2V, a new unified framework for video editing. Our framework is training-free, highly cost-effective, and can be applied to any I2V model. To perform video editing with high precision, we propose a two-stage approach to first edit the initial frame of the source video and then condition an image-to-video (I2V) model with the initial frame. Comprehensive experiments have shown that our method achieves outstanding outcomes across a broad spectrum of applications and shows a high level of controllability.

7 Limitations

Inaccurate Edit from Image Editing Models. As our method relies on an initial frame edit, the image editing models are used. However, the current state-of-the-art models are not mature enough to perform accurate edits consistently [32]. For example, in the subject-driven video editing task, we found that AnyDoor [11] requires several tries to get a good editing result. Efforts are required in manually picking a good edited frame. We expect that in the future better image editing models will minimize such effort.

Limited ability of I2V models. We found that the results from our method cannot follow the source video motion if the motion is fast (e.g. billiard balls hitting each other at full speed) or complex (e.g. a person clipping her hair). One possible reason is that the current popular I2V models are generally trained on slow-motion videos, such that lacking the ability to regenerate fast or complex motion even with motion guidance. We anticipate that the presence of a robust I2V model can address this issue.

8 Potential Negative Impacts

Misinformation spread and Privacy violations. As our technique allows for object manipulation, it can produce highly realistic yet completely fabricated videos of one individual or subject. There is a risk that harmful actors could exploit our system to generate counterfeit videos to disseminate false information. Moreover, the ability to create convincing counterfeit content featuring individuals without their permission undermines privacy protections, possibly leading to the illicit use of a person’s likeness for harmful purposes and damaging their reputation. These issues are similarly present in DeepFake technologies. To mitigate the risk of misuse, one proposed solution is the adoption of unseen watermarking, a method commonly used to tackle such concerns in image generation.

References

1. An, J., Zhang, S., Yang, H., Gupta, S., Huang, J.B., Luo, J., Yin, X.: Latent-shift: Latent diffusion with temporal shift for efficient text-to-video generation. arXiv preprint arXiv:2304.08477 (2023) [4](#)
2. Avrahami, O., Lischinski, D., Fried, O.: Blended diffusion for text-driven editing of natural images. In: Proceedings of the IEEE/CVF Conference on Computer Vision and Pattern Recognition. pp. 18208–18218 (2022) [4](#), [7](#)
3. Bai, J., He, T., Wang, Y., Guo, J., Hu, H., Liu, Z., Bian, J.: Uniedit: A unified tuning-free framework for video motion and appearance editing. arXiv preprint arXiv:2402.13185 (2024) [2](#), [3](#), [4](#), [8](#), [10](#)
4. Bar-Tal, O., Chefer, H., Tov, O., Herrmann, C., Paiss, R., Zada, S., Ephrat, A., Hur, J., Li, Y., Michaeli, T., et al.: Lumiere: A space-time diffusion model for video generation. arXiv preprint arXiv:2401.12945 (2024) [3](#)
5. Blattmann, A., Rombach, R., Ling, H., Dockhorn, T., Kim, S.W., Fidler, S., Kreis, K.: Align your latents: High-resolution video synthesis with latent diffusion models. In: Proceedings of the IEEE/CVF Conference on Computer Vision and Pattern Recognition. pp. 22563–22575 (2023) [4](#)
6. Brooks, T., Holynski, A., Efros, A.A.: Instructpix2pix: Learning to follow image editing instructions. In: CVPR (2023) [3](#), [4](#), [10](#), [12](#), [24](#)
7. Ceylan, D., Huang, C.H.P., Mitra, N.J.: Pix2video: Video editing using image diffusion (2023) [5](#), [10](#)
8. Chen, H., Xia, M., He, Y., Zhang, Y., Cun, X., Yang, S., Xing, J., Liu, Y., Chen, Q., Wang, X., et al.: Videocrafter1: Open diffusion models for high-quality video generation. arXiv preprint arXiv:2310.19512 (2023) [4](#)
9. Chen, H., Zhang, Y., Cun, X., Xia, M., Wang, X., Weng, C., Shan, Y.: Videocrafter2: Overcoming data limitations for high-quality video diffusion models. arXiv preprint arXiv:2401.09047 (2024) [2](#)
10. Chen, S., Xu, M., Ren, J., Cong, Y., He, S., Xie, Y., Sinha, A., Luo, P., Xiang, T., Perez-Rua, J.M.: Gentrion: Delving deep into diffusion transformers for image and video generation. arXiv preprint arXiv:2312.04557 (2023) [4](#)
11. Chen, X., Huang, L., Liu, Y., Shen, Y., Zhao, D., Zhao, H.: Anydoor: Zero-shot object-level image customization. arXiv preprint arXiv:2307.09481 (2023) [3](#), [4](#), [7](#), [10](#), [11](#), [13](#), [16](#), [24](#)
12. Chen, X., Wang, Y., Zhang, L., Zhuang, S., Ma, X., Yu, J., Wang, Y., Lin, D., Qiao, Y., Liu, Z.: Seine: Short-to-long video diffusion model for generative transition and prediction. arXiv preprint arXiv:2310.20700 (2023) [3](#), [4](#), [10](#), [21](#)
13. Chen, Y., Lai, Y.K., Liu, Y.J.: Cartoongan: Generative adversarial networks for photo cartoonization. In: 2018 IEEE/CVF Conference on Computer Vision and Pattern Recognition. pp. 9465–9474 (2018). <https://doi.org/10.1109/CVPR.2018.00986> [4](#)
14. Cheng, J., Xiao, T., He, T.: Consistent video-to-video transfer using synthetic dataset. arXiv preprint arXiv:2311.00213 (2023) [7](#)
15. Cong, Y., Xu, M., Simon, C., Chen, S., Ren, J., Xie, Y., Perez-Rua, J.M., Rosenhahn, B., Xiang, T., He, S.: Flatten: optical flow-guided attention for consistent text-to-video editing. arXiv preprint arXiv:2310.05922 (2023) [2](#), [3](#), [5](#), [10](#), [11](#), [12](#)
16. Dhariwal, P., Nichol, A.: Diffusion models beat gans on image synthesis. *Advances in neural information processing systems* **34**, 8780–8794 (2021) [5](#)
17. Esser, P., Chiu, J., Atighehchian, P., Granskog, J., Germanidis, A.: Structure and content-guided video synthesis with diffusion models. In: Proceedings of the

- IEEE/CVF International Conference on Computer Vision. pp. 7346–7356 (2023) [2](#)
18. Gatys, L.A., Ecker, A.S., Bethge, M.: A neural algorithm of artistic style. CoRR [abs/1508.06576](#) (2015), <http://arxiv.org/abs/1508.06576> [3](#), [4](#), [7](#), [10](#), [11](#), [12](#), [24](#)
 19. Ge, S., Nah, S., Liu, G., Poon, T., Tao, A., Catanzaro, B., Jacobs, D., Huang, J.B., Liu, M.Y., Balaji, Y.: Preserve your own correlation: A noise prior for video diffusion models. In: Proceedings of the IEEE/CVF International Conference on Computer Vision. pp. 22930–22941 (2023) [4](#)
 20. Geyer, M., Bar-Tal, O., Bagon, S., Dekel, T.: Tokenflow: Consistent diffusion features for consistent video editing. arXiv preprint arxiv:2307.10373 (2023) [2](#), [3](#), [5](#), [7](#), [10](#), [11](#), [12](#)
 21. Ghiasi, G., Lee, H., Kudlur, M., Dumoulin, V., Shlens, J.: Exploring the structure of a real-time, arbitrary neural artistic stylization network. CoRR [abs/1705.06830](#) (2017), <http://arxiv.org/abs/1705.06830> [7](#)
 22. Gu, J., Wang, Y., Zhao, N., Fu, T.J., Xiong, W., Liu, Q., Zhang, Z., Zhang, H., Zhang, J., Jung, H., Wang, X.E.: Photoswap: Personalized subject swapping in images (2023) [4](#), [7](#)
 23. Gu, Y., Zhou, Y., Wu, B., Yu, L., Liu, J.W., Zhao, R., Wu, J.Z., Zhang, D.J., Shou, M.Z., Tang, K.: Videoswap: Customized video subject swapping with interactive semantic point correspondence. arXiv preprint (2023) [2](#)
 24. Guo, Y., Yang, C., Rao, A., Wang, Y., Qiao, Y., Lin, D., Dai, B.: Animatediff: Animate your personalized text-to-image diffusion models without specific tuning. arXiv preprint arXiv:2307.04725 (2023) [4](#)
 25. Gupta, A., Yu, L., Sohn, K., Gu, X., Hahn, M., Fei-Fei, L., Essa, I., Jiang, L., Lezama, J.: Photorealistic video generation with diffusion models. arXiv preprint arXiv:2312.06662 (2023) [4](#)
 26. Ho, J., Chan, W., Saharia, C., Whang, J., Gao, R., Gritsenko, A., Kingma, D.P., Poole, B., Norouzi, M., Fleet, D.J., et al.: Imagen video: High definition video generation with diffusion models. arXiv preprint arXiv:2210.02303 (2022) [4](#)
 27. Ho, J., Jain, A., Abbeel, P.: Denoising diffusion probabilistic models. *Advances in neural information processing systems* **33**, 6840–6851 (2020) [4](#)
 28. Ho, J., Salimans, T.: Classifier-free diffusion guidance. arXiv preprint arXiv:2207.12598 (2022) [8](#), [10](#)
 29. Ho, J., Salimans, T., Gritsenko, A., Chan, W., Norouzi, M., Fleet, D.J.: Video diffusion models. arXiv:2204.03458 (2022) [4](#)
 30. Horn, B.K., Schunck, B.G.: Determining optical flow. *Artificial intelligence* **17**(1-3), 185–203 (1981) [8](#)
 31. Ku, M., Li, T., Zhang, K., Lu, Y., Fu, X., Zhuang, W., Chen, W.: Imagenhub: Standardizing the evaluation of conditional image generation models. arXiv preprint arXiv:2310.01596 (2023) [4](#)
 32. Ku, M., Li, T., Zhang, K., Lu, Y., Fu, X., Zhuang, W., Chen, W.: Imagenhub: Standardizing the evaluation of conditional image generation models. In: The Twelfth International Conference on Learning Representations (2024), <https://openreview.net/forum?id=OuV9ZrkQlc> [11](#), [16](#)
 33. Ku, W.F., Siu, W.C., Cheng, X., Chan, H.A.: Intelligent painter: Picture composition with resampling diffusion model (2022) [4](#), [7](#)
 34. Li, T., Ku, M., Wei, C., Chen, W.: Dreamedit: Subject-driven image editing (2023) [4](#), [7](#)

35. Liang, F., Wu, B., Wang, J., Yu, L., Li, K., Zhao, Y., Misra, I., Huang, J.B., Zhang, P., Vajda, P., et al.: Flowvid: Taming imperfect optical flows for consistent video-to-video synthesis. arXiv preprint arXiv:2312.17681 (2023) [2](#)
36. Liu, S., Zhang, Y., Li, W., Lin, Z., Jia, J.: Video-p2p: Video editing with cross-attention control. arXiv preprint arXiv:2303.04761 (2023) [2](#)
37. Löttsch, W., Reimann, M., Büfemeyer, M., Semmo, A., Döllner, J., Trapp, M.: Wise: Whitebox image stylization by example-based learning. ECCV (2022) [4](#), [7](#)
38. Mokady, R., Hertz, A., Aberman, K., Pritch, Y., Cohen-Or, D.: Null-text inversion for editing real images using guided diffusion models. In: Proceedings of the IEEE/CVF Conference on Computer Vision and Pattern Recognition. pp. 6038–6047 (2023) [3](#), [5](#)
39. Molad, E., Horwitz, E., Valevski, D., Acha, A.R., Matias, Y., Pritch, Y., Leviathan, Y., Hoshen, Y.: Dreamix: Video diffusion models are general video editors. arXiv preprint arXiv:2302.01329 (2023) [4](#)
40. Nichol, A.Q., Dhariwal, P., Ramesh, A., Shyam, P., Mishkin, P., Mcgrew, B., Sutskever, I., Chen, M.: Glide: Towards photorealistic image generation and editing with text-guided diffusion models. In: International Conference on Machine Learning. pp. 16784–16804. PMLR (2022) [4](#), [7](#)
41. OpenAI: Video generation models as world simulators, <https://openai.com/research/video-generation-models-as-world-simulators> [4](#)
42. Qi, C., Cun, X., Zhang, Y., Lei, C., Wang, X., Shan, Y., Chen, Q.: Fatezero: Fusing attentions for zero-shot text-based video editing. arXiv:2303.09535 (2023) [5](#)
43. Radford, A., Kim, J.W., Hallacy, C., Ramesh, A., Goh, G., Agarwal, S., Sastry, G., Askell, A., Mishkin, P., Clark, J., et al.: Learning transferable visual models from natural language supervision. In: International conference on machine learning. pp. 8748–8763. PMLR (2021) [10](#)
44. Ren, W., Yang, H., Zhang, G., Wei, C., Du, X., Huang, S., Chen, W.: Consisti2v: Enhancing visual consistency for image-to-video generation. arXiv preprint arXiv:2402.04324 (2024) [3](#), [4](#), [10](#), [21](#)
45. Rombach, R., Blattmann, A., Lorenz, D., Esser, P., Ommer, B.: High-resolution image synthesis with latent diffusion models. In: Proceedings of the IEEE/CVF conference on computer vision and pattern recognition. pp. 10684–10695 (2022) [2](#), [4](#), [5](#)
46. Sohl-Dickstein, J., Weiss, E., Maheswaranathan, N., Ganguli, S.: Deep unsupervised learning using nonequilibrium thermodynamics. In: International conference on machine learning. pp. 2256–2265. PMLR (2015) [4](#)
47. Song, J., Meng, C., Ermon, S.: Denoising diffusion implicit models. arXiv preprint arXiv:2010.02502 (2020) [3](#), [5](#), [10](#)
48. Suvorov, R., Logacheva, E., Mashikhin, A., Remizova, A., Ashukha, A., Silvestrov, A., Kong, N., Goka, H., Park, K., Lempitsky, V.: Resolution-robust large mask inpainting with fourier convolutions. arXiv preprint arXiv:2109.07161 (2021) [4](#), [7](#)
49. Tumanyan, N., Geyer, M., Bagon, S., Dekel, T.: Plug-and-play diffusion features for text-driven image-to-image translation. In: Proceedings of the IEEE/CVF Conference on Computer Vision and Pattern Recognition (CVPR). pp. 1921–1930 (June 2023) [4](#), [5](#)
50. Tumanyan, N., Geyer, M., Bagon, S., Dekel, T.: Plug-and-play diffusion features for text-driven image-to-image translation. In: Proceedings of the IEEE/CVF Conference on Computer Vision and Pattern Recognition. pp. 1921–1930 (2023) [10](#)
51. Wang, Q., Bai, X., Wang, H., Qin, Z., Chen, A.: Instantid: Zero-shot identity-preserving generation in seconds. arXiv preprint arXiv:2401.07519 (2024) [3](#), [4](#), [7](#), [10](#), [11](#), [14](#), [24](#)

52. Wang, X., Yuan, H., Zhang, S., Chen, D., Wang, J., Zhang, Y., Shen, Y., Zhao, D., Zhou, J.: Videocomposer: Compositional video synthesis with motion controllability. *Advances in Neural Information Processing Systems* **36** (2024) [4](#)
53. Wang, Y., Chen, X., Ma, X., Zhou, S., Huang, Z., Wang, Y., Yang, C., He, Y., Yu, J., Yang, P., et al.: Lavie: High-quality video generation with cascaded latent diffusion models. *arXiv preprint arXiv:2309.15103* (2023) [2](#), [4](#)
54. Wu, B., Chuang, C.Y., Wang, X., Jia, Y., Krishnakumar, K., Xiao, T., Liang, F., Yu, L., Vajda, P.: Fairy: Fast parallelized instruction-guided video-to-video synthesis. *arXiv preprint arXiv:2312.13834* (2023) [2](#), [5](#)
55. Wu, J.Z., Ge, Y., Wang, X., Lei, S.W., Gu, Y., Shi, Y., Hsu, W., Shan, Y., Qie, X., Shou, M.Z.: Tune-a-video: One-shot tuning of image diffusion models for text-to-video generation. In: *Proceedings of the IEEE/CVF International Conference on Computer Vision*. pp. 7623–7633 (2023) [2](#), [3](#), [10](#), [11](#), [12](#)
56. Xia, W., Zhang, Y., Yang, Y., Xue, J.H., Zhou, B., Yang, M.H.: Gan inversion: A survey. *IEEE Transactions on Pattern Analysis and Machine Intelligence (TPAMI)* (2022) [3](#)
57. Xing, J., Xia, M., Zhang, Y., Chen, H., Wang, X., Wong, T.T., Shan, Y.: Dynamicafter: Animating open-domain images with video diffusion priors. *arXiv preprint arXiv:2310.12190* (2023) [4](#)
58. Yang, S., Zhou, Y., Liu, Z., , Loy, C.C.: Rerender a video: Zero-shot text-guided video-to-video translation. In: *ACM SIGGRAPH Asia Conference Proceedings* (2023) [5](#)
59. Zeng, Y., Wei, G., Zheng, J., Zou, J., Wei, Y., Zhang, Y., Li, H.: Make pixels dance: High-dynamic video generation. *arXiv preprint arXiv:2311.10982* (2023) [4](#)
60. Zhang, K., Mo, L., Chen, W., Sun, H., Su, Y.: Magicbrush: A manually annotated dataset for instruction-guided image editing. *NeurIPS dataset and benchmark track* (2023) [4](#)
61. Zhang, L., Rao, A., Agrawala, M.: Adding conditional control to text-to-image diffusion models (2023) [14](#)
62. Zhang, S., Wang, J., Zhang, Y., Zhao, K., Yuan, H., Qin, Z., Wang, X., Zhao, D., Zhou, J.: I2vgen-xl: High-quality image-to-video synthesis via cascaded diffusion models. *arXiv preprint arXiv:2311.04145* (2023) [2](#), [3](#), [4](#), [10](#), [21](#)
63. Zhou, D., Wang, W., Yan, H., Lv, W., Zhu, Y., Feng, J.: Magicvideo: Efficient video generation with latent diffusion models. *arXiv preprint arXiv:2211.11018* (2022) [4](#)

Supplementary Material

A Discussion on Model Implementation Details

When adapting our AnyV2V to various I2V generation models, we identify two sets of hyperparameters that are crucial to the final video editing results. They are (1) selection of U-Net decoder layers (l_1 , l_2 and l_3) to perform convolution, spatial attention and temporal attention injection and (2) Injection thresholds τ_{conv} , τ_{sa} and τ_{ta} that control feature injections to happen in specific diffusion steps. In this section, we provide more discussions and analysis on the selection of these hyperparameters.

A.1 U-Net Layers for Feature Injection

To better understand how different layers in the I2V denoising U-Net produce features during video sampling, we perform a visualization of the convolution, spatial and temporal attention features for the three candidate I2V models I2VGen-XL [62], ConsistI2V [44] and SEINE [12]. Specifically, we visualize the average activation values across all channels in the output feature map from the convolution layers, and the average attention scores across all attention heads and all tokens (i.e. average attention weights for all other tokens attending to the current token). The results are shown in Figure 6.

According to the figure, we observe that the intermediate convolution features from different I2V models show similar characteristics during video generation: earlier layers in the U-Net decoder produce features that represent the overall layout of the video frames and deeper layers capture the high-frequency details such as edges and textures. We choose to set $l_1 = 4$ for convolution feature injection to inject background and layout guidance to the edited video without introducing too many high-frequency details. For spatial and temporal attention scores, we observe that the spatial attention maps tend to represent the semantic regions in the video frames while the temporal attention maps highlight the foreground moving subjects (e.g. the running woman in Figure 6). One interesting observation for I2VGen-XL is that its spatial attention operations in deeper layers almost become hard attention, as the spatial tokens only attend to a single or very few tokens in each frame. We propose to inject features in decoder layers 4 to 11 ($l_2 = l_3 = \{4, 5, \dots, 11\}$) to preserve the semantic and motion information from the source video.

A.2 Ablation Analysis on Feature Injection Thresholds

We perform additional ablation analysis using different feature injection thresholds to study how these hyperparameters affect the edited video.

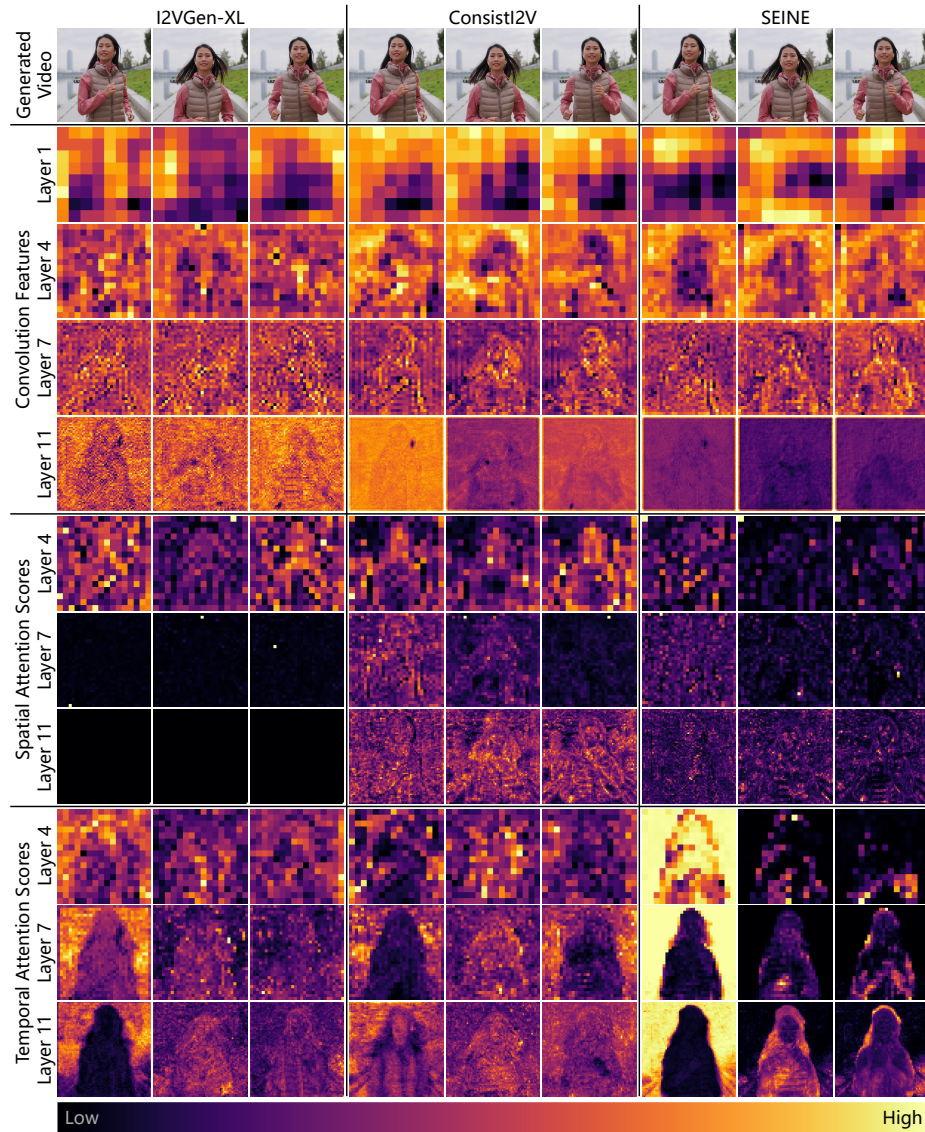


Fig. 6: Visualizations of the convolution, spatial attention and temporal attention features during video sampling for I2V generation models’ decoder layers. We feed in the DDIM inverted noise to the I2V models such that the generated videos (first row) are reconstructions of the source video.

Effect of Spatial Injection Thresholds τ_{conv}, τ_{sa} We study the effect of disabling spatial feature injection or using different τ_{conv} and τ_{sa} values during video editing and show the qualitative results in Figure 7. We find that when spatial feature injection is disabled, the edited videos fail to fully adhere to the layout and motion from the source video. When spatial feature injection

Source $\tau_{c,s} = 0$ $\tau_{c,s} = 0.2T$ $\tau_{c,s} = 0.5T$ $\tau_{c,s} = 0.7T$ $\tau_{c,s} = T$

Fig. 7: Hyperparameter study on spatial feature injection. We find that $\tau_{sa} = 0.2T$ is the best setting for maintaining the layout and structure in the edited video while not introducing unnecessary visual details from the source video. $\tau_{c,s}$ represents τ_{conv} and τ_{sa} . (Editing prompt: *teddy bear running*. Videos clickable in Adobe Acrobat.)

thresholds are too high, the edited videos are corrupted by the high-frequency details from the source video (e.g. textures from the woman’s down jacket in Figure 7). Setting $\tau_{conv} = \tau_{sa} = 0.2T$ achieves a desired editing outcome for our experiments.

Effect of Temporal Injection Threshold τ_{ta} We study the hyperparameter of temporal feature injection threshold τ_{ta} in different settings and show the results in Figure 8. We observe that in circumstances where $\tau_{ta} < 0.5T$ (T is the total denoising steps), the motion guidance is too weak that it leads to only partly aligned motion with the source video, even though the motion itself is logical and smooth. At $\tau_{ta} > 0.5T$, the generated video shows a stronger adherence to the motion but distortion occurs. We employ $\tau_{ta} = 0.5T$ in our experiments and find that this value strikes the perfect balance on motion alignment, motion consistency, and video fidelity.

Source $\tau_{ta} = 0$ $\tau_{ta} = 0.2T$ $\tau_{ta} = 0.5T$ $\tau_{ta} = 0.7T$ $\tau_{ta} = T$

Fig. 8: Hyperparameter study on temporal feature injection. We find that $\tau_{ta} = 0.5T$ to be the optimal setting as it balances motion alignment, motion consistency, and video fidelity. (Editing prompt: *darth vader walking*. Videos clickable in Adobe Acrobat.)

A.3 Backbones Performance

Among the three backbones of our framework, We found that AnyV2V (I2VGen-XL) tends to be the most robust model both qualitatively and quantitatively. It has a good generalization ability to produce consistent motions in the video with high visual quality. AnyV2V (ConsistI2V) can generate consistent motion, but

sometimes the watermark would appear due to its data used during the training stage, thus harming the visual quality. AnyV2V (SEINE)’s generalization ability is relatively weaker but still produces consistent and high-quality video if the motion is simple enough, such as a person walking. One interesting property of our framework is that although in some cases the motion does not fully align with the source video, it produces video with high motion consistency and reasonable motion that is highly similar to the source video, indicating the flexibility of how the video can be edited while maintaining the video fidelity.

B Human Evaluation Dataset

Our human evaluation dataset contains in total of 89 samples. For prompt-based editing, we employed InstructPix2Pix [6] to compose the examples. Topics include swapping objects, adding objects, and removing objects. For subject-driven editing, we employed AnyDoor [11] to replace objects with reference subjects. For Neural Style Transfer, we employed NST [18] to compose the examples. For identity manipulation, we employed InstantID [51] to compose the examples. See Table 4 for the statistic.

Table 4: Number of entries for Video Editing Evaluation Dataset

Category	Number of Entries	Image Editing Models Used
Prompt-based Editing	45	InstructPix2Pix [6]
Reference-based Style Transfer	20	NST [18]
Identity Manipulation	13	InstantID [51]
Subject-driven Editing	11	AnyDoor [11]
Total	89	